Measurement of Hole Volume in Amorphous Polymers Using Positron Spectroscopy

H. A. Hristov,*,† B. Bolan,† A. F. Yee,† L. Xie,‡ and D. W. Gidley‡

Departments of Materials Science & Engineering and Physics, The University of Michigan, Ann Arbor, Michigan 48109

Received May 16, 1996; Revised Manuscript Received September 12, 1996[⊗]

ABSTRACT: Positron annihilation lifetime spectroscopy (PALS) measurements, in the temperature range 110−480 K, are given for three linear, amorphous polymers. Based on these measurements, a method is proposed for evaluating the hole volume in amorphous thermoplastics. Our studies show that hole volume is composed of static and dynamic components. We demonstrate that the dynamic component, which is a result of the thermal vibrations of the molecular chains, is strongly correlated to thermodynamic volume/density fluctuations. The static hole volume is interpreted as "frozen-in" fluctuations, which are manifested as nanometer-sized flaws in the packing of molecular chains. The results from PALS measurements reported in our work are in very good agreement with results from small-angle X-ray scattering measurements.

Introduction

The quality of molecular packing, which can be modified by different technological operations, influences a number of important properties of amorphous polymers. It is well known that changes in molecular arrangements can significantly alter mechanical response, thermal stability, durability, and other materials properties.[1−3] Thus, knowledge of molecular configurations has significant practical importance. The availability of detailed structural information is also important from a fundamental point of view, since realistic models of polymer behavior must be based on a sound description of the chain packing and should be able to account for different microstructural changes.

Despite considerable effort, progress in this area is hampered by difficulties in determining the microstructure of amorphous polymers (and all other disordered materials as well). Results from commonly used techniques such as X-ray scattering and electron microscopy lack sufficient precision and are often inconclusive, which may lead to nonunique data interpretation. It is worth noting that, despite numerous studies and even more numerous debates,[4−11] the chain packing on a scale smaller than the radius of gyration of the molecular coils is not well known. To further advance our understanding of the molecular order in amorphous polymers, it is necessary to obtain diverse structural information by using a wide range of experimental methods.

In the last two decades, positron annihilation lifetime spectroscopy (PALS) has been used in various studies of polymers,[12,13] and the PALS response has been shown to be correlated to the microstructure of the polymers under study.[12−14] After entering the polymer, a positron may exist as a "free" positron (lifetime ∼0.3−0.5 ns) or form a bound state (positronium, Ps). The singlet state ($S = 0$) of Ps, parapositronium (p-Ps), has a lifetime of 125 ps, while the triplet state ($S = 1$) of Ps, orthopositronium (o-Ps), has a lifetime of 142 ns in vacuum. In amorphous polymers, o-Ps is trapped in regions of lower electron density, which are usually interpreted as "holes" or "microvoids". The observed o-Ps lifetime in the holes is reduced to several nanoseconds because the annihilation is facilitated by the overlap of the positron wave function with molecular electrons (the so-called "pick-off" mechanism). In such a way, the lifetime of o-Ps depends on the hole size,[15−17] while its relative intensity is interpreted to be proportional to the positronium formation probability and, hence, the number density of holes.[14,18,19] Since the efficiency of chain packing should affect the size and/or the number of holes, the PALS method can be very useful in studying molecular configurations in amorphous polymers.

To use PALS as a quantitative structural probe, one needs to resolve some ambiguities in the data interpretation and understand the underlying physical processes controlling the dynamics of the holes probed by positrons. It is also necessary to devise a general procedure for evaluating the hole volume fraction in glassy polymers. The interpretation of PALS data, and the hole volume computations as well,[14−20] is frequently based on the "free volume" concept.[21−23] This approach can lead to significant difficulties in obtaining an unambiguous, quantitative description of PALS results since (a) free volume models are not rigorously quantitative, even for liquids composed of simple molecules (for more details, see the discussion in ref 24); (b) there is no unique definition of free volume;[18−20] and (c) the precise relationship between the hole volume probed by the positrons and the free volume defined by the various models is not clear.

In a recent study, we proposed a simple procedure for evaluating the hole volume in amorphous polycarbonate (PC), based on the measurements of the thermal expansion and/or mechanical deformation.[25] The aim of the present study is to propose a more general approach for derivation of the hole volume fraction in amorphous polymers, based on measurements of the macroscopic and microscopic thermal expansions in a wide temperature range. An attempt is also made to clarify the physical processes controlling the changes of the hole volume in linear thermoplastics and to correlate the PALS results with those from other structural methods. To pursue these goals, we have used PALS to investigate three amorphous polymers: polystyrene (PS), poly(methyl methacrylate) (PMMA), and PC. All three polymers are important commercial thermoplastics, and there exists a considerable amount of data regarding their structure and properties.[26−28] Polystyrene is a

† Department of Materials Science & Engineering.
‡ Department of Physics.
[⊗] Abstract published in *Advance ACS Abstracts,* November 15, 1996.

S0024-9297(96)00719-X CCC: $12.00

brittle, low entanglement density polymer; polycarbonate is a tough and ductile material with high density of molecular entanglements. The mechanical properties and molecular arrangements of PMMA are intermediate between those of PS and PC. The three polymers either are noncrystallizable (depending on tacticity) or crystallize extremely slowly in the absence of solvents, which allows prolonged measurements above the glass transition temperature without development of a crystalline phase.

Experimental Section

Materials. I. Polycarbonate. The polycarbonate specimens were prepared from materials from two different sources, differing only in their end groups.

(i) Sample PC1. High-purity laboratory-grade polycarbonate made by the Dow Chemical Co. ($M_w \approx 58\,000$ g/mol, $M_n \approx 27\,300$ g/mol, as measured by GPC calibrated by a polystyrene standard). This PC is capped by *tert*-butylphenol endgroups. The samples were prepared by compression molding of pellets dried in a vacuum chamber at 110 °C for about 12 h. A 25 μCi ^{22}Na source was deposited between two identical PC samples (0.75 in. × 0.75 in. × 0.25 in.). Temperature changes in the range 23−200 °C were provided by a small heating tape wrapped around the polymer/source/polymer sandwich using a temperature controller, which maintains temperatures stable to ±0.5 °C. Each PALS data point was obtained by first heating the sandwich to 165 °C (15 °C above the glass transition temperature, T_g) and then cooling down (5 °C/min) to the desired temperature to erase the thermal history of previous runs.

(ii) Sample PC2. Commercial-grade polycarbonate resin made by the General Electric Co. (LEXAN, Mw ≈ 59 700 g/mol, $M_n \approx 29\,600$ g/mol, GPC polystyrene standard). This PC is capped by phenol end groups. The compression-molded sample was dried in a vacuum chamber at 110 °C for about 12 h and then heated to and held at 165 °C (15 °C above T_g) for 40 min to erase any previous thermal and mechanical history. A 30 μCi ^{22}Na positron source, deposited on the surface of an aluminum disk, was placed on the surface of the specimen under study. The sandwich composed of the positron source and the polymer was heated by the same heating tape as above; however, the data were collected sequentially, starting from room temperature and monotonically increasing to 200 °C.

II. Polystyrene. The polystyrene samples were also prepared from materials from two different sources.

(i) Sample PS1. High-purity monodispersed polystyrene ($M_w = 600\,000$ g/mol, $M_w/M_n = 1.1$) produced by Polysciences, Inc. The positron source used for these measurements is the same source used for specimen PC2, and the heating was sequentially increased.

(ii) Sample PS2. Commercial-grade polystyrene, made by Mitsubishi Kasei Co. ($M_w \approx 260\,000$ g/mol, $M_w/M_n \approx 2.5$). For these measurements, a 25 μCi ^{22}Na positron source was deposited between two identical specimens (similar to the PC1 case), and before each measurement the sandwich was heated above T_g.

III. Poly(methyl methacrylate). The PMMA specimen was prepared from a commercial-grade material ($M_w \approx 280\,000$ g/mol, $M_w/M_n \approx 2.5$). The PALS measurements were performed using the same source as for specimens PC2 and PS1 and sequential heating. All measurements were done in air.

Specimens PC2, PS1, and PMMA were measured also in the temperature range −160 to +20 °C, using a low-temperature chamber cooled by liquid nitrogen. The measurements were performed stepwise in a sequential manner (from low to high temperatures); the temperature was maintained within ±0.5 °C at each step.

The linear coefficients of thermal expansion of the materials were measured by using either a Perkin-Elmer or a TA Instruments thermomechanical analyzer. The calorimetric glass transition temperatures were determined by using a Perkin-Elmer differential scanning calorimeter at a heating rate of 10 °C/min.

PALS. The positron lifetime spectra were obtained by a conventional fast-timing coincidence method (see ref 25). Signals from the start and stop detectors, consisting of plastic scintillators coupled to photomultipliers (Amperex XP2020 with 5563 bases), were processed by two constant fraction differential discriminators (CFDDs, Ortec583), with the start energy window nominally set for the ^{22}Na 1.28 MeV nuclear γ-ray (indicating the birth of a positron) and the stop set for the 511 keV annihilation γ-rays. The digitized signals were fed into a micro-VAX station (Digital Model 3100) which also performs data analysis. The spectrum full width at half-maximum of the prompt time resolution curve was 300 ps, as determined by a ^{60}Co source. Since the o-Ps intensities from the polymers change during the irradiation by the e^+ source, prior to the actual measurements the materials were irradiated for 12 h. This procedure (charging) ensures virtually constant I_3 for the next several days.

Analysis. The spectrum was fitted to three exponential components: the respective lifetimes and relative intensities, together with the time resolution, were determined by the FORTRAN program PFPOSFIT.[29] The first (τ_1) and second (τ_2) components, which can be associated with p-Ps and bulk positron annihilations respectively, were found to be unaffected by the temperature change and thus will not be considered further. The long-lived third (τ_3) component and its relative intensity (I_3), which is associated with the annihilation of o-Ps trapped in the holes, was sensitive to the structural changes induced by the temperature increase.

A simple spherical hole model[15,16] is used to relate τ_3 with the radius (R) of the hole where the o-Ps localizes. If one assumes that, inside the hole where o-Ps localizes, it decays at its vacuum rate ($\lambda_{o-Ps} = 1/142$ ns^{-1}), and o-Ps only penetrates a small distance (ΔR) into the wall of the hole, where it annihilates at the spin-averaged rate ($\lambda_{spin} = 1/(4 \times 0.125) + 3/(4 \times 142)$ ns^{-1}) as it is surrounded by an electron cloud, the average o-Ps annihilation rate of such a localized o-Ps can be given by

$$\tau^{-1} = \lambda_{spin} G + \lambda_{o-Ps}(1 - G) \tag{1}$$

where $G = 1 - R/(R + \Delta R) + 1/2\pi \sin[2\pi R/(R + \Delta R)]$ is the quantum mechanical probability that o-Ps is in the electron cloud, R is the radius of the hole, and ΔR is the o-Ps penetration depth into the wall of the hole wherein the o-Ps annihilates at the spin-averaged lifetime of 0.5 ns. The best fit of the combined experimental data[16,17,30] gives $\Delta R = 1.61$ Å.

The relative intensity, I_3, is commonly assumed to be proportional to the number density of the holes. The hole volume V_h is then proportional to the product of the average volume of a single hole, $v_h = 4\pi R^3/3$ (R is computed from eq 1) and I_3, i.e.,

$$V_h = C v_h I_3 \tag{2}$$

where C is a normalization constant which remains to be determined. (A similar approach has been used previously,[14,18−20] wherein the normalization constant is derived on the basis of free volume considerations.) Without analyzing the physical processes leading to changes in the hole volume, it is assumed that an increase of the product $v_h I_3$ corresponds to "expansion" of the hole volume and vice versa. With this assumption, it is possible to formally introduce a coefficient of thermal expansion of the hole volume. However, this does not mean that the holes expand in a fashion similar to gas bubbles; rather, the changes of the surroundings lead to changes in their size and/or number density. In the final section of this article, we will discuss the physical origins of the hole volume in amorphous polymers and its changes with temperature.

As in our previous work,[25] the total volume of the specimen will be divided into two parts:

$$V = V_h + V_b \tag{2a}$$

where V_b is bulk volume, which cannot be sampled by o-Ps. From this definition, it follows that the bulk volume is

composed of the volume occupied by the molecular chains and the volume of those holes, which cannot be detected by PALS. Let us further express the thermal expansivities of the total (macroscopic) volume in the vicinity of T_g as

$$\alpha_1 = \frac{1}{V(T_1)}\left(\frac{\partial V}{\partial T}\right)_{P=\text{const}} \qquad T \le T_g \tag{3}$$

$$\alpha_2 = \frac{1}{V(T_2)}\left(\frac{\partial V}{\partial T}\right)_{P=\text{const}} \qquad T \ge T_g \tag{4}$$

where $T_1 = T_g - \Delta$, $T_2 = T_g + \Delta$, Δ is an infinitesimally small positive number with dimension of temperature. From the definitions of T_1 and T_2 it follows that the differences between $V(T_g)$ and $V(T_1)$ and/or $V(T_2)$ are vanishingly small. (In the text below, it is assumed that the volume changes are effected at constant external pressure; therefore, this will not be explicitly stated. It is also assumed, for simplicity, that the glass transition is a pointwise process and that the changes of the total, hole, and bulk volumes are reasonably linear in its vicinity. See also Results.)

In a similar fashion, the thermal expansivities of the hole (microscopic) volume are

$$\alpha_{h1} = \frac{1}{V_h(T_1)}\frac{\partial V_h}{\partial V} \qquad T \le T_g \tag{5}$$

$$\alpha_{h2} = \frac{1}{V_h(T_2)}\frac{\partial V_h}{\partial T} \qquad T \ge T_g \tag{6}$$

and the thermal expansivities of the bulk volume are

$$\alpha_{b1} = \frac{1}{V_b(T_1)}\frac{\partial V_b}{\partial T} \qquad T \ge T_g \tag{7}$$

$$\alpha_{b2} = \frac{1}{V_b(T_2)}\frac{\partial V_b}{\partial T} \qquad T \ge T_g \tag{8}$$

By using the above-defined quantities and eq 2a, the hole volume fraction at the glass transition is written as (see Appendix I)

$$F_h(T_g) = \frac{V_h(T_g)}{V(T_g)} = \frac{\alpha_1 - \alpha_{b1}}{\alpha_{h1} - \alpha_{b1}} \qquad T \le T_g \tag{9}$$

when T_g is approached from low temperatures and as

$$F_h(T_g) = \frac{V_h(T_g)}{V(T_g)} = \frac{\alpha_2 - \alpha_{b2}}{\alpha_{h2} - \alpha_{b2}} \qquad T \ge T_g \tag{10}$$

when determined from the high-temperature region.

Since F_h is nonnegative, it is clear, from (9) and (10), that $\alpha_{b1} \le \alpha_1$ and $\alpha_{b2} \le \alpha_2$ (α_b is always smaller than the respective α_h). Furthermore, taking into account that F_h is a continuous function, it is evident that

$$\frac{\alpha_1 - \alpha_{b1}}{\alpha_{h1} - \alpha_{b1}} = \frac{\alpha_2 - \alpha_{b2}}{\alpha_{h2} - \alpha_{b2}} \tag{11}$$

A fundamental problem of deriving $F_h(T_g)$ via eqs 9 and 10 arises from the fact that we cannot directly measure the expansivities of the bulk volume (α_{b1} and α_{b2}). As discussed previously,[25] one way to circumvent this problem is to take the expansivities of the bulk volume to be much smaller than those of the hole volume, i.e., $\alpha_{h1} \gg \alpha_{b1}$ and $\alpha_{h2} \gg \alpha_{b2}$, based on the assumption that changes in the total volume are predominantly due to the changes in the hole volume. A phenomenological basis for this assumption is the fact that the hole volume (microscopic) expansivities are more than an order of magnitude larger than the respective expansivities of the total (macroscopic) volume (see Results). Thus, by assuming $\alpha_b \approx 0$ in the temperature range immediately above and below the T_g, the hole volume fraction can be approximated by

$$F_h(T_g) \approx \alpha_1/\alpha_{h1} \quad \text{or} \quad F_h(T_g) \approx \alpha_2/\alpha_{h2} \tag{12}$$

As discussed with regard to eq 11 the continuity of F_h and eqs 12 requires an equality of the ratios of the total and hole volumes at temperatures immediately below and above the glass transition. In general, the ratios of the experimentally measured total (macro-) and hole (micro-) expansivities (which we shall call "characteristic ratios") can be categorized into three possible cases.

Case I:

$$\alpha_1/\alpha_{h1} \approx \alpha_2/\alpha_{h2}$$

The assumption that the bulk expansivities are negligible ($\alpha_b \approx 0$) leads to eq 12 for normalizing the experimental measurements (see above). It can be shown that, in general, eq 12 is an upper bound estimate of the hole volume fraction (i.e., $F_{hmax} = \alpha/\alpha_h$), and smaller values will be obtained for $\alpha_{b1} \neq 0$ and $\alpha_{b2} \neq 0$ by using (9)−(11), as long as the bulk volume expansivities conform to

$$\alpha_1/\alpha_{b1} = \alpha_2/\alpha_{b2} \tag{13}$$

The relationship between the bulk and total expansivities can be expressed as

$$\alpha_b = A\alpha \qquad 0 \le A \le 1 \tag{14}$$

where A is a constant that will depend on the properties of the particular material. By using (14), eqs 9 and 10 are written as

$$F_h = \frac{F_{hmax} - AF_{hmax}}{1 - AF_{hmax}} \tag{15}$$

where the product AF_{hmax} is also a materials constant, i.e., $B = AF_{hmax}$. As will be shown, F_{hmax} is smaller than 0.1, thus eq 15 can be approximated by

$$F_h \approx F_{hmax} - B \tag{16}$$

Case II:

$$\alpha_1/\alpha_{h1} < \alpha_2/\alpha_{h2}$$

In this situation, the range of the possible solutions is bounded by

$$0 \le F_h(T_g) \le F_{hmax}(T_g)$$

where $F_{hmax}(T_g)$ is obtained from

$$F_{hmax}(T_g) = \alpha_1/\alpha_{h1} \tag{17}$$

Physically, it means that the bulk expansivity just below T_g can be ignored ($\alpha_{b1} \approx 0$), i.e., the polymer's response is similar to case I in the same temperature range; however, the bulk expansion at high temperatures is not negligible in comparison to α_2 ($\alpha_{b2} \neq 0$; α_{b2} is always much smaller than α_{h2}).

Case III:

$$\alpha_1/\alpha_{h1} > \alpha_2/\alpha_{h2} \tag{17}$$

In this case, the bulk expansivities both below and above the glass transition are not negligible with respect to the total expansivities. An estimate of the hole volume fraction can be obtained by assuming that, in the vicinity of T_g, the bulk expansivities are close to each other, e.g. $\alpha_{b1} \approx \alpha_{b2} > 0$. It can be shown (Appendix II) that this assumption leads to the following normalization expression:

$$F_{hmax}(T_g) = \Delta\alpha/\Delta\alpha_h \tag{18}$$

where $\Delta\alpha$ and $\Delta\alpha_h$ are the discontinuities of the respective

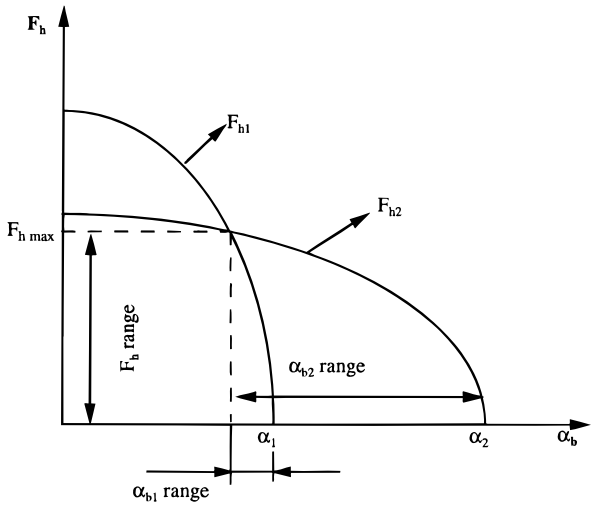

Figure 1. Graphical solutions of eqs 9 and 10 for a case III polymer (see text for details).

expansivities at the glass transition, i.e., $\Delta\alpha = \alpha_2 - \alpha_1$ and $\Delta\alpha_h = \alpha_{h2} - \alpha_{h1}$. It is clear that case III is more general than case I since we do not require negligible bulk expansivities. The hole volume fraction computed by using (18) is an upper estimate, and even higher estimates can be obtained if we assume $\alpha_{b1} > \alpha_{b2}$, but the latter is most probably never realized in polymeric materials. In Figure 1 are shown the solutions of eqs 9 and 10 (designated by F_{h1} and F_{h2}) in graphical form for a case III polymer as functions of α_{b1} and α_{b2}, respectively. The physically meaningful ranges of F_h, α_{b1}, and α_{b2} values are also shown. F_h values higher than the value indicated by F_{hmax} in the figure (computed from eq 18) are obtained only if $\alpha_{b1} > \alpha_{b2}$. Similarly to case I (eq 16), it can be shown that $F_h \approx F_{hmax} - B$, where B is a material's constant.

Results

In the derivation of eqs 9−18,we did not take into account two experimental facts: (a) the glass transition is not a point on the temperature axis but rather a region and (b) immediately below the glass transition all polymers exhibit volume relaxation (physical aging) with relaxation times comparable to the PALS measurement times. In Figure 2b,c are shown schematically the experimentally observed deviations from the ideal behavior (Figure 2a). It is also shown that, in the vicinity of the glass transition, the experimental curves can be approximated with two lines (broken lines). By using this two-line approximation, the derivation of $V_h(T_g)$, α_{h1}, and α_{h2} is the same as in the idealized glass transition case depicted in Figure 2a (eqs 5 and 6). The V_h temperature dependence for PS and PMMA showed deviations similar to that shown in Figure 2b, while the PC material's behavior is close to that depicted in Figure 2c.

The linear thermal expansion of both PC samples was found to be $(8 \pm 0.5) \times 10^{-5}$/K for $T < T_g$ (150 °C); for the PS specimens, the respective value is $(7.7 \pm 0.5) \times 10^{-5}$/K ($T$ < 110 °C), and for PMMA it is $(9 \pm 0.5) \times 10^{-5}$/K ($T$ < 105 °C). However we were not able to obtain sufficiently accurate data for temperatures higher than the glass transition. Thus, for the high-temperature region, we will use the values given in Table 1 (obtained from refs 26−28).

The values of the coefficients of thermal expansion of the hole volume were obtained from the PALS measurements by using eqs 5 and 6.

Polycarbonate. (i) Specimen PC1. Hole volume expansion coefficients:

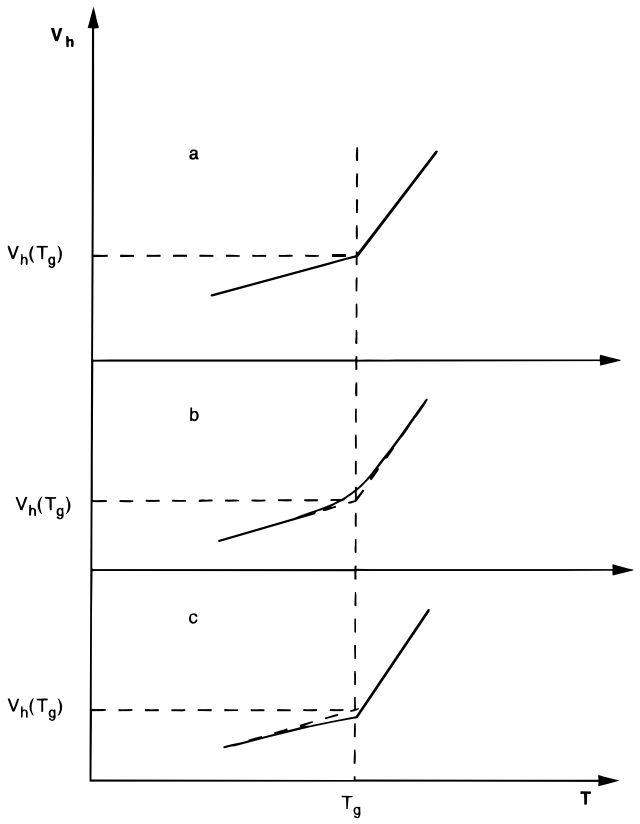

Figure 2. Ideal glass transition (a) and the experimentally observed deviations, resulting from smearing (b) and physical aging (c).

Table 1. Volumetric Expansion Coefficients

material	$T < T_g$ (K^{-1})	$T > T_g$ (K^{-1})
polycarbonate	$\alpha_1 = 2.55 \times 10^{-4}$	$\alpha_2 = 5.74 \times 10^{-4}$
polystyrene	$\alpha_1 = 2.3 \times 10^{-4}$	$\alpha_2 = 5.14 \times 10^{-4}$
PMMA	$\alpha_1 = 2.7 \times 10^{-4}$	$\alpha_2 = 5.8 \times 10^{-4}$

$$\alpha_{h1} = (29 \pm 1) \times 10^{-4}/\text{K}$$
$$\alpha_{h2} = (62 \pm 1.5) \times 10^{-4}/\text{K}$$

Characteristic ratios:

$$\alpha_1/\alpha_{h1} = 0.087 \qquad \alpha_2/\alpha_{h2} = 0.093$$

(ii) Specimen PC2. Hole volume expansion coefficients:

$$\alpha_{h1} = (28 \pm 1) \times 10^{-4}/\text{K}$$
$$\alpha_{h2} = (60 \pm 1.5) \times 10^{-4}/\text{K}$$

Characteristic ratios:

$$\alpha_1/\alpha_{h1} = 0.0914 \qquad \alpha_2/\alpha_{h2} = 0.096$$

The results from the PALS measurements show that the respective thermal expansion coefficients of the hole volume of the two materials are very close to each other both below and above the glass transition. Keeping in mind the experimental errors, it is fair to say that the respective characteristic ratios below and above T_g are also reasonably close to each other. Based on these results, we conclude that the two polycarbonates can be nominally categorized as case I polymers, and the respective $F_h(T_g)$ were computed as averages of the characteristic ratios, which leads to ~9.0% for PC1 and ~9.4% for PC2. The experimental error in determining F_h is estimated to be no more than ±0.3% for all of the

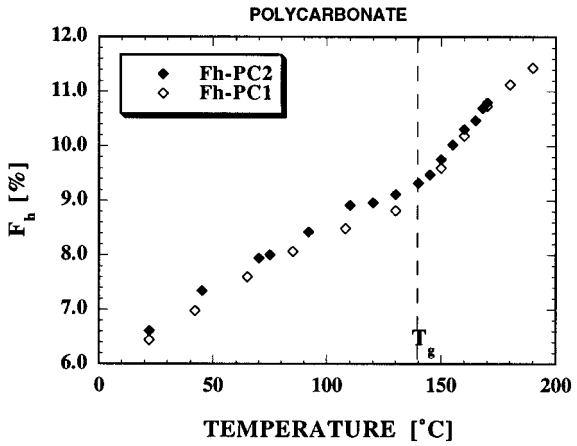

Figure 3. Temperature changes of the hole volume fraction in polycarbonates.

Table 2. Hole Volume Fractions at T_g

polymer	F_{hmax} (%)[a]	F_{hmin} (%)[a]
PC1	9	
PC2	9.4	7.9
PS1	5	3.3
PS2	4.4	
PMMA	5.3	4

[a] The experimental error in F_{hmax} and F_{hmin} is ±0.3%.

materials studied in the present work. In the evaluation of the F_h error, we assumed that the uncertainty in the macroscopic expansion coefficients (Table 1) is negligible in comparison to the errors in deriving α_h. In Figure 3 the temperature changes of the hole volume fractions of the two PC specimens are shown, and in Table 2 the results from all materials are summarized. Figure 3 demonstrates that the proposed normalization is independent of the experimental setup and that the hole volume changes are characteristic of the particular material. While mathematically the range of possible solutions is $0 \le F_h \le F_{hmax}$, physically it is highly unlikely that the bulk volume expansivities (α_b) will be both comparable to the total volume expansivities and yet satisfy eq 13. Thus, it is reasonable to accept that, if the experimental values of the expansion coefficients conform to case I (see Analysis section), then the bulk expansivities are negligible and eq 12 gives a realistic evaluation of the entire hole volume fraction. Our previous measurements of the hole volume fraction using mechanical deformation (instead of thermal expansion) gave $F_h \approx 7\%$[25] for specimen PC2 at room temperature, while the present result is $F_h \approx 6.5\%$ at the same temperature (Figure 3). This can be regarded as additional evidence that the normalization procedure described above is physically reasonable.

Polystyrene. (i) Specimen PS1. Hole volume expansion coefficients:

$$\alpha_{h1} = (28 \pm 1) \times 10^{-4}/\mathrm{K}$$
$$\alpha_{h2} = (85 \pm 2) \times 10^{-4}/\mathrm{K}$$

Characteristic ratios:

$$\alpha_1/\alpha_{h1} = 0.083 \qquad \alpha_2/\alpha_{h2} = 0.06$$

(ii) Specimen PS2. Hole volume expansion coefficients:

$$\alpha_{h1} = (31 \pm 1) \times 10^{-4}/\mathrm{K}$$
$$\alpha_{h2} = (88 \pm 2) \times 10^{-4}/\mathrm{K}$$

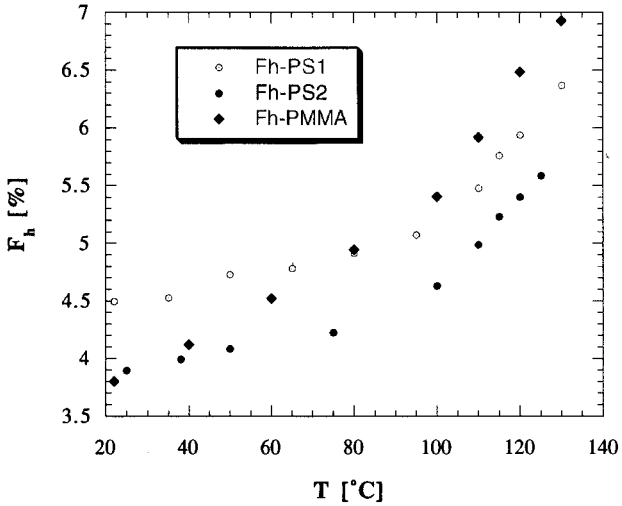

Figure 4. Temperature changes of the hole volume fractions in polystyrenes and PMMA.

Characteristic ratios:

$$\alpha_1/\alpha_{h1} = 0.075 \qquad \alpha_2/\alpha_{h2} = 0.058$$

Similar to the PC measurements, the results from the two PS show that their respective expansion coefficients below and above T_g are sample independent; however, the characteristic ratios below the glass transition are higher than those obtained from the high-temperature region. According to the categorization in the Analysis section, PS is a case III material, and the hole volume fractions were therefore computed from

$$F_{hmax}(T_g) = \Delta\alpha/\Delta\alpha_h$$

The hole volume fractions at T_g are reasonably close to each other (PS1, $F_h(T_g) \approx 5\%$; PS2, $F_h(T_g) \approx 4.4\%$); however, the overlap between the two curves is not as good as for the polycarbonate specimens (Figure 4 vs Figure 3). Taking into account the considerable difference in molecular weights and weight distributions of the two PS materials, some differences between the two curves are to be expected. By using the $F_h(T_g)$ value, one can compute that the bulk volume expansivity is $\alpha_b \approx 9 \times 10^{-5}$/K.

PMMA. Hole volume expansion coefficients:

$$\alpha_{h1} = (38 \pm 1) \times 10^{-4}/\mathrm{K}$$
$$\alpha_{h2} = (98 \pm 2) \times 10^{-4}/\mathrm{K}$$

Characteristic ratios:

$$\alpha_1/\alpha_{h1} = 0.071 \qquad \alpha_2/\alpha_{h2} = 0.059$$

The results show that the PALS response of PMMA is analogous to that of the PS samples, i.e., it is a case III material, too. The hole volume fraction computed from the discontinuities of the expansion coefficients (eq 18) is comparable to that of the polystyrene ($F_h(T_g) \approx 5.3\%$; Table 2). Similarly, the deduced bulk volume expansion is $\alpha_b \approx 8 \times 10^{-5}$/K.

The $F_h(T_g)$ values, computed using eqs 12 and 18, are in the expected range for this class of amorphous materials. Nonetheless, they are upper bound estimates, and mathematically the hole volume fraction could be close to 0% at T_g if $\alpha_b \approx \alpha$ in eqs 9 and 10. Clearly, the latter is far from physical reality, but it illustrates that our results would be more meaningful

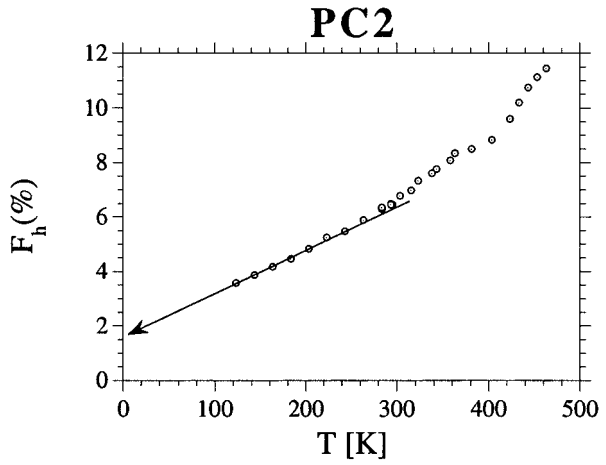

Figure 5. Static hole volume (the arrow indicates extrapolation toward 0 K) of PC.

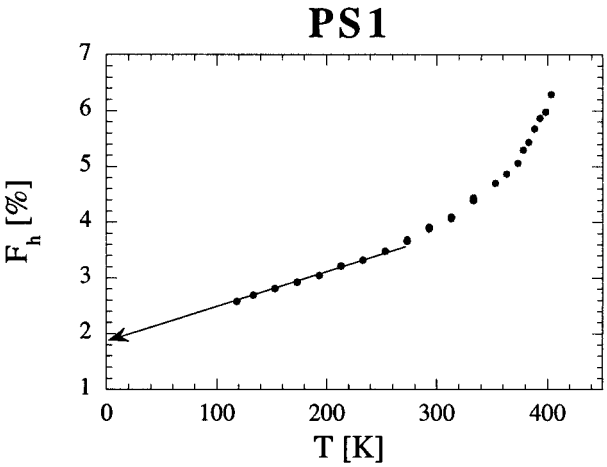

Figure 6. Static hole volume (the arrow indicates extrapolation toward 0 K) of polystyrene.

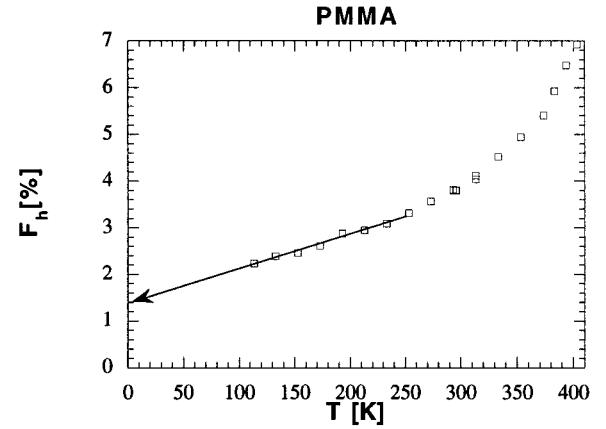

Figure 7. Static hole volume (the arrow indicates extrapolation toward 0 K) of PMMA.

if we could obtain realistic estimates for the lower bounds of the respective F_h values.

In an effort to set lower limits on F_h, the specimens PC2, PS1 and PMMA were measured in the low-temperature range down to 110 K. In Figures 5−7, the deduced changes in the hole volume fractions for the three polymers are shown (the respective changes of τ_3 and I_3 are given in Appendix III). As demonstrated in the figures, the low-temperature portions of the curves are nearly linear and can be extrapolated toward 0 K. The extrapolated values of the hole volume fractions, which we shall call "static hole volume", of the three polymers are in the range 1−2%. Since F_h cannot be negative, its lowest possible value at 0 K is 0%; thus, by shifting vertically downward the curves by ∼1.5%, ∼1.7%, and ∼1.3% (the maximum possible values of the constant B in eq 16 for the respective polymers), one can obtain estimates of the lowest bounds of the hole volume fractions at each temperature. The hole volume fractions, designated by $F_{hmin}(T_g)$ in Table 2, were determined from the shifted curves. As a result of the general approach used in the evaluation of F_h instead of using a fixed value at each temperature we are able to determine only a range of possible values. However, the assumption $F_h(0\ K) \approx 0\%$ implies that the chain packing somehow becomes almost perfect at 0 K, which is obviously incorrect for amorphous polymers. Based on these considerations, it is reasonable to assume that the actual F_h values at different temperatures are close to the curves normalized by using eq 12 or 18 and depicted in Figures 3−7.

Discussion

As shown in the Analysis section, if the expansivity of the bulk volume is negligible (eqs 9 and 10), the hole volume fraction is easily derived. In deducing the amount of "open" volume, it is necessary to account for the fact that the positrons cannot sample all of the microscopic "holes" present in the material. Keeping in mind that the electron density is lower in the space between the molecular chains than the electron density of the space occupied by the individual chains (or van der Waals (V_W) volume[26]), it is reasonable to accept that the o-Ps will localize in the former. However, if the interchain holes are smaller than ∼1.9 Å in radius and/or if they open and close with frequencies higher than $\sim 1 \times 10^9$ Hz, the o-Ps cannot localize and annihilate there. (The various versions of PALS analysis based on the free volume approach[14,18−20] assume that the o-Ps uniformly probes the entire "free volume", which includes small holes and rapidly vibrating holes. None of these works provides experimental evidence in support of such an assumption.) Thus, the bulk volume V_b, introduced in eqn 2a, is composed of the V_W volume (the major part of V_b) and voids too small or too "fast" to allow positronium localization. We shall henceforth refer to these as "undetectable" hole volume. Due to the covalent bonding along the chain, the thermal expansion of the V_W should be very small for all polymers;[26] however, the contribution from the undetectable hole volume may not be negligible and will depend on the molecular structure and packing of the particular polymer, and the temperature range under study as well. In other words, the question is whether or not the changes detected by PALS are a sufficiently good representation of the changes of the interchain volume with temperature, given the relatively weak interchain interactions. Assuming that the thermal expansion coefficient of the undetectable hole volume is similar to that of the experimentally detected hole volume changes, we arrive at a straightforward conclusion that eq 12 approximates the entire hole volume (detectable and undetectable by PALS). If the above assumption is not valid, then there is no simple relationship between the experimentally measured changes of V_h and the changes of the undetectable holes. The presence of these holes will lead to an increase in the effective bulk expansivity, which in the case of PS and PMMA is only 3−4 times lower than the total volume expansivity in the glassy state. An attempt to normalize the hole volume from the α_l/α_{hl} ratio will result in ∼80% overestimation. This example underscores the impor-

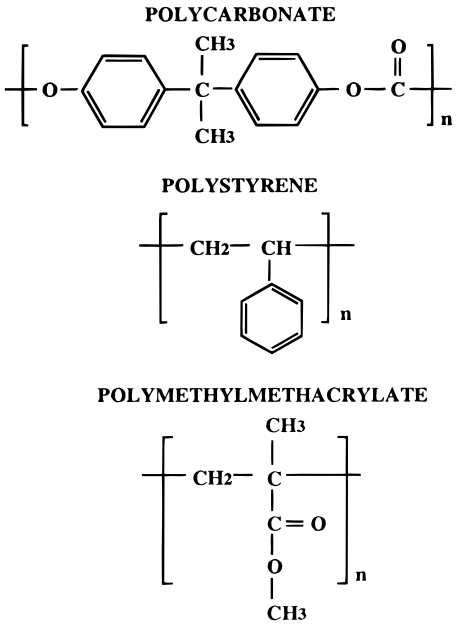

Figure 8. Monomer structures of PC, PS, and PMMA.

tance of measuring the expansivities over a sufficiently wide temperature range.

The difference in the characteristic responses of PC (case I) on the one hand and PS and PMMA (case III) on the other is most probably rooted in the peculiarities of their molecular structures. As shown in Figure 8, the PS and PMMA repeat units are characterized by bulky side groups, which could lead to complex topologies of the interchain (hole) volume. In comparison, the polycarbonate chain is relatively smooth, probably resulting in a much simpler interchain volume topology; thus, its sampling by positrons is possibly more effective. In this respect the characteristic ratio behavior (case I, II, or III) appears to be indicative of the topology of the interchain space of the particular polymer. This question needs further studies on a wider range of polymeric materials.

A comparison of the results in Table 2 with previous measurements shows that, for polycarbonate, the hole volume fraction computed from PALS data, using a simplified representation of the free volume fraction[31] (8%), is lower than our values (9−9.4% at T_g), while the free volume fraction computed from the PVT data is a little higher (∼10% at T_g).[31] Another free volume-based interpretation of PALS data reports a room temperature value of 6.23%,[32] which is almost identical to our values. An attempt to normalize F_h from low-tempeature PALS measurements of PC has led to unreasonably high values: ∼19% at room temperature.[33] According to our analysis, values of 8% at T_g and 6.2% at T_{room} for PC are within the $F_{hmin}-F_{hmax}$ range (Table 2), an indication that the assumptions made in our work and in refs 31 and 32 are compatible with the physical processes underlying the thermal expansion in PC. Our F_h values for polystyrene are 20−30% lower than the results from the free volume-based computations, 4−4.5% vs ∼6%[19,34] at room temperature. The PALS-determined F_h values in ref 19 are consistently lower than the theoretical values computed from the Simha−Somcinsky (SS) free volume model[19] at temperatures lower than T_g. It seems that a normalization based on free volume computation overestimates the hole volume fraction in polystyrene. Our $F_h(T_g)$ values, the values in refs 19, 31, 32, and 34, and the SS values are several times larger than the "universal" free volume fraction value of 2.5% at T_g.[24]

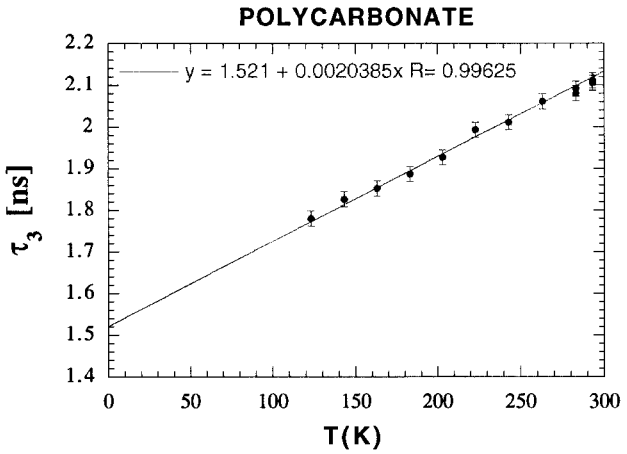

Figure 9. Changes of the o-Ps lifetime at low temperatures; specimen PC2.

To understand the physical origins of the "static hole volume" or $F_h(T = 0)$ (see Results), it is necessary to account for different types of defects in the molecular packing. Since the chains of all linear thermoplastics with sufficiently high molecular mass are entangled and have two ends, it seems natural to start with these types of packing imperfections. If we take polycarbonate as an example, a chain with $M_n \approx 25\,000$ g/mol is composed of ∼100 monomer units. By using the volume of the unit cell of the PC crystal, the density of the crystalline material, the density, and the thermal expansion of the amorphous PC, it can be shown that a monomer occupies ∼352 Å^3 at room temperature[35] and ∼323 Å^3 at 0 K. As shown in Figure 9, extrapolation of τ_3 to 0 K gives a value of ∼1.52 ns (the size of the error bars shown in Figure 8 is typical for all of our measurements). From eq 1, the radius of the static hole is ∼2.31 Å, and the volume of the average static hole is $v_h(0\ K) \approx 52$ Å^3. The entanglement molecular mass of PC is ∼2500 g/mol,[36] i.e., one entanglement per ∼10 monomer units, which leads to ∼10 packing defects per chain (about eight entanglements and two ends). This simple calculation assumes that an entanglement point can be treated as a topological defect, which is not necessarily correct. If we further assume that the volume of a single defect is $v_{def}(0\ K) \approx v_h(0\ K)$, such an assumption leads to ∼520 Å^3 for the total volume of defects per chain. The total chain volume is $\sim 3.2 \times 10^4$ Å^3; thus, the static holes occupy ∼1.6% of the volume of the material at 0 K. This excellent agreement with the hole volume fraction extrapolated to 0 K determined in Figure 4 is probably fortuitous. Similar computations yield values of 0.12−0.15% for the PS and PMMA materials, i.e., an order of magnitude less than the respective F_h values at 0 K. Apparently, the contribution to the static hole volume from entanglements and chain ends is rather insignificant.

To identify the source of the static hole volume, it may be fruitful to analyze the temperature dependence of V_h. First, we should account for the fact that the extra hole volume generated at higher temperatures (which we will call "dynamic hole volume") results from the thermal vibrations of the molecular chains. (Based on this definition, it is interesting to note that polycarbonate, which is the most ductile of the three polymers, possesses the highest dynamic hole volume at room temperature.) These vibrations induce volume/density fluctuations, and their measurable quantity is the mean square deviation. The standard thermodynamic theory defines the mean square of the fluctuations of an equilibrium fluid at temperature T as[37]

$$\langle \delta V^2 \rangle = k_B T (\partial V / \partial P)_T = k_B T \chi_T V \qquad (19)$$

where k_B is the Boltzman constant, χ_T is the isothermal compressibility of the respective material, and V is the volume of the subsystem under consideration. (In the text below, the mean square of the volume/density fluctuations per unit volume will be denoted by FL, e.g., FL = $\langle \delta V^2 \rangle / V$). Equation 19 demonstrates that, at equilibrium, the temperature change of FL is governed by the product $T\chi_T$. As shown in Figure 10 for PMMA, the temperature change of the normalized hole volume can be divided into three quasilinear regions. The temperature range above T_g corresponds to the "liquid" state of the polymer, i.e., the material is close to thermodynamic equilibrium, and eq 19 should be applicable. In contrast, all amorphous polymers are in a metastable state at temperatures below T_g; thus, eq 19 is not valid for this temperature range. (There is no accepted theory describing nonequilibrium FL at present.) The change of the normalized FL(T) computed from eq 19 is also plotted in Figure 10 (solid line). It is evident that the change of the hole volume in the high-temperature T region is controlled by equilibrium thermodynamics. The temperature designated by T_β in Figure 10 roughly corresponds to the maximum of the loss modulus, at $T < T_g$, when measured by dynamical mechanical spectroscopy (DMS) at 1 Hz.[24] This peak is usually associated with relatively small scale segmental or side group motions known as secondary relaxations or "β-relaxations"[24] (primary or α-relaxation being the glass transition). In the temperature range $T_g - T_\beta$, the change of the $V_h(T)$ is proportional to $T\chi_{T_g}$ rather than $T\chi_T$. Almost identical changes in FL(T) have been observed in studies of amorphous PMMA when measured by small-angle X-ray scattering (SAXS).[38−40] The same is valid for Figures 4 and 5 when compared to the SAXS measurements of the respective polymers.[38−41]

For a one-component system, the X-ray intensity at wavevector $q \to 0$ is related to the density fluctuations by[9]

$$I(0) = \rho^2(\langle \delta V^2 \rangle / V) = \rho^2 k_B T \chi_T \qquad (20)$$

where ρ is the scattering density of the system. For temperatures between T_g and T_β, the experimentally observed intensity follows $I(0) \approx \rho^2 k_B T \chi_{T_g}$ rather than eq 20.[38−41] Since ρ is a relatively slowly varying (with temperature) function, the observed temperature changes are controlled by $T\chi_T$ or $T\chi_{T_g}$, which explains the correspondence between SAXS and PALS measurements.

On the basis of the above discussion and the correspondence with SAXS results, it is evident that there is a correlation of the dynamic hole volume with the thermodynamic volume/density fluctuations. It should be emphasized, however, that the two methods (PALS and SAXS) do not measure the same quantities. To clarify this point, let us consider a fluid system with macroscopic (average) density ρ_0 at a fixed temperature $T > 0$. The thermodynamic fluctuations will produce local deviations from ρ_0, and at a fixed time some small portions of the specimen will possess densities higher than ρ_0 (FL+), while in other locations the densities will be lower than ρ_0 (FL−) (some authors call the two different types of fluctuations p-type and n-type[42,43]). As a result of the dynamic nature of the process, the two types of fluctuations annihilate mutually in random locations throughout the specimen, while new FL+ and FL− are generated in other locations,[42,43] and the average number density of the fluctuations does not change with time.[38] Taking into account the fact that X-ray intensity is proportional to $\Delta\rho^2$, the results from SAXS measurements will represent a spatial average of both FL+ and FL−. Due to the specifics of the formation and localization of o-Ps, a PALS measurement gives an average of the holes located predominantly within FL−, which are large enough and slow enough (fluctuate with frequencies $<10^9$ Hz) to localize o-Ps. In so doing, PALS results do not fully account for all the possible fluctuations in the system. On the other hand, the limit $q \to 0$ for the SAXS measurements means that mostly longitudinal, long-wavelength (low-frequency) vibrations contribute to the density fluctuations defined by eq 20.[39] It is reasonable to expect that a large portion of the n-type, "soft" vibrational modes will be registered by PALS.

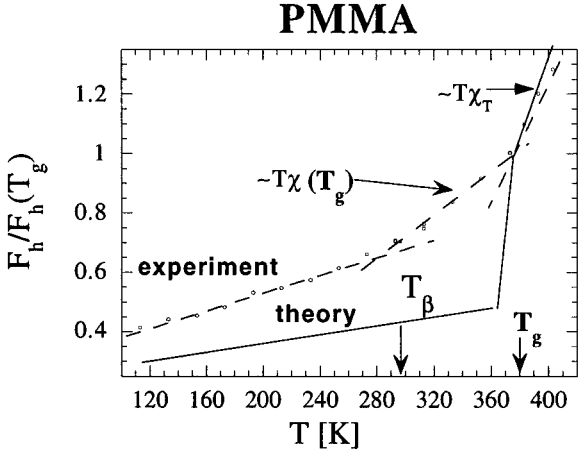

Figure 10. Temperature changes of the normalized hole volume fraction in PMMA (dashed lines) and the normalized thermodynamic fluctuations (eq 19; solid line).

In the vicinity of the glass transition, the thermal energy will increase the number density of the long-range (wavelength larger than several repeat units) molecular motions. Taking into account that the mean square vibrational amplitude is proportional to $1/\omega$ (ω is vibrational frequency),[44] the long-wavelength vibrations will be the main contributor to the thermal expansion. Under these conditions, the assumption that the temperature change of V_h can account for the largest part of the volumetric expansion of the polymeric materials at temperatures close to T_g (see Analysis) should provide a satisfactory description of the process. In addition, the origin of the static hole volume can be explained on the basis of the presence of thermodynamic fluctuations as follows. It is widely accepted that part of the FL "freezes" when the liquid is cooled through the glass transition,[38,39,42,43] which leads to the change of slope in the microscopic and macroscopic volume dependence on the temperature. While details of this process are not known at present, it is evident that, after cooling to 0 K, the "frozen" FL− represents a major part of the open volume left in the amorphous polymer.

It is useful to attempt to correlate the size of the density fluctuations deduced from PALS measurements and from theoretical predictions (eq 19). The thermodynamic theory does not give a frequency spectrum for the fluctuations, but a rough comparison can still be made by introducing some simplifications. From the results reported above, one can compute that the volume of an average hole is ~100 Å^3. Let us use $F_h = 5\%$, and macroscopic (average) density $\rho_0 = 1$ g/cm^3 at 400 K. It is evident that the density of the material without the

holes is 1.05 g/cm^3. It is convenient to "partition" the specimen into elementary volumes (V_e) with sizes equal to 2000 Å^3 and assume that each of these volumes contains one hole at any moment of time. Now let us take an arbitrary V_e and split it into two equal parts, left and right. The dynamics of generation and annihilation of volume/density fluctuations inside V_e can be simplified by assuming that the hole belonging to this particular V_e spends some time (longer than 2−3 ns) in the left part and after that jumps to the right part. After residing there longer than 2−3 ns, it jumps back to the left part and so on. Under these conditions, the density of each of the two parts (with volumes 1000 Å^3) will vary with time as $\rho_0 \pm 5\%$ (1 ± 0.05 g/cm^3). To continue further, it is convenient to rewrite eq 19 as

$$\langle \delta\rho^2 \rangle / {\rho_0}^2 = k_B T \chi_T / V \tag{21}$$

where $\langle \delta\rho^2 \rangle$ is the second moment of the density fluctuations, and V is the volume of the subsystem. By solving eq 21 for V using $\rho_0 = 1$ g/cm^3, $T = 400$ K, $\chi_T = 5 \times 10^{-4}$/MPa (these values are close to the respective materials parameters for PS and PMMA), and $\langle \delta\rho^2 \rangle = (0.05 \text{ g/cm}^3)^2$, one obtains $V \approx 1200$ Å^3. In view of the considerable simplifications introduced in the computations above, this value is surprisingly close to the estimate obtained on the basis of the PALS results (1000 Å^3). For some other polymers, the values computed from PALS and from eqs 19−21 may not be as close, but it is apparent that PALS measurements can be interpreted on the basis of the theory of thermodynamic volume/density fluctuations.

Conclusions

On the basis of PALS measurements of linear thermoplastics over a wide temperature range, we propose a new method for the evaluation of the lower and upper bounds of the hole volume fraction at each temperature. The distinction between earlier concepts of "free" volume and hole volume measured by PALS is discussed within a model wherein the volume of the polymer is divided into two components: hole volume, which can be probed by positronium (V_h), and bulk volume, which is not accessible to o-Ps (V_b). The bulk volume includes the van der Waals volume plus voids too small or too rapidly oscillating to be detectable with PALS. The hole volume, probed by positronium, includes some parts of the conventionally defined free volume but as a rule is different from the latter. A comparison of the macroscopic and microscopic expansivities show that different polymers exhibit different behaviors, which is most probably related to the topology of the interchain space. The measurements are interpreted in a scheme wherein the hole volume detected by PALS is composed of static and dynamic components. It is shown that the static component can be identified with "frozen-in" thermodynamic volume/density fluctuations. The analysis indicates that, for high molecular weight linear polymers, the contribution to the hole volume from packing imperfections such as molecular entanglements (assuming that the entanglements can be regarded as topological defects) and chain ends is negligible. The dynamic part of the hole volume is a result of the thermal vibrations, and its temperature change is strongly correlated to the temperature changes of equilibrium or nonequilibrium (depending on the temperature range) thermodynamic volume/density fluctuations. The PALS results reported in the present work are in very good agreement with SAXS studies of the density fluctuations in amorphous PC, PS, and PMMA.[38−41]

Acknowledgment. We thank Mark Scalsey for technical assistance. This research is supported in part by the U.S. Department of Energy, Grant No. DE-FGO2-88ER45366, the National Science Foundation, Grant No. ECS-9402599, and the University of Michigan. B.B. is supported by the Air Force Palace Knights Fellowship and Grant AFOSR No. F496W-95-1-0037.

Appendix I

By differentiating eq 2a with respect to the temperature (at constant pressure), one obtains

$$\frac{\partial V}{\partial T} = \frac{\partial V_h}{\partial T} + \frac{\partial V_b}{\partial T} \tag{1.1}$$

Further, both sides of eq 1.1 are divided by $V(T_i)$, and by using eqs 3 and 4 one obtains

$$\alpha_i = \frac{1}{V(T_i)} \frac{\partial V_h}{\partial T} + \frac{1}{V(T_i)} \frac{\partial V_b}{\partial T} \tag{1.2}$$

where $i = 1$ and 2. Equation 1.2 can be rewritten as

$$\alpha_i = \frac{V_h(T_i)/V_h(T_i)}{V(T_i)} \frac{\partial V_h}{\partial T} + \frac{V_b(T_i)/V_b(T_i)}{V(T_i)} \frac{\partial V_b}{\partial T} \tag{1.3}$$

Keeping in mind that when $\Delta \to 0$, $V(T_i) \to V(T_g)$, and $V_h(T_i) \to V_h(T_g)$, eq 1.3 becomes

$$\alpha_i = F_h(T_g) \frac{1}{V_h(T_i)} \frac{\partial V_h}{\partial T} + [1 - F_h(T_g)] \frac{1}{V_b(T_i)} \frac{\partial V_b}{\partial T} \tag{1.4}$$

By using eqs 1.4 and 5−8, one obtains eqs 9 and 10.

Appendix II

For a case III polymer, e.g., $\alpha_{b1} \approx \alpha_{b2} = \alpha_b \neq 0$, eqs 9 and 10 are written as

$$F_h(T_g) = \frac{\alpha_1 - \alpha_b}{\alpha_{h1} - \alpha_b}$$
$$F_h(T_g) = \frac{\alpha_2 - \alpha_b}{\alpha_{h2} - \alpha_b} \tag{2.1}$$

The two equations in (2.1) can be rearranged in the following manner:

$$\alpha_b = \frac{\alpha_1 - F_h \alpha_{h1}}{1 - F_h} \tag{2.2}$$

$$\alpha_b = \frac{\alpha_2 - F_h \alpha_{h2}}{1 - F_h} \tag{2.3}$$

After subtracting (2.2) from (2.3), the result is

$$\alpha_2 - \alpha_1 = F_h(\alpha_{h2} - \alpha_{h1}) \tag{2.4}$$

By introducing $\Delta\alpha = \alpha_2 - \alpha_1$ and $\Delta\alpha_h = \alpha_{h2} - \alpha_{h1}$, eq 2.4 is written as

$$F_h(T_g) = \Delta\alpha / \Delta\alpha_h \tag{2.5}$$

Appendix III

In Figures 11−13 are shown the temperature changes of the o-Ps lifetimes and intensities for the three

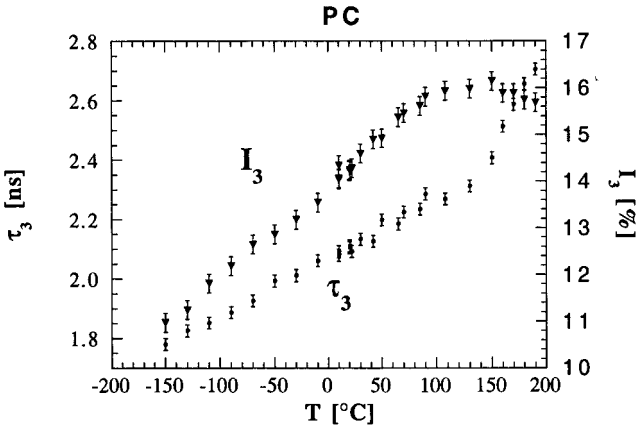

Figure 11. Temperature changes of the o-Ps lifetime and intensity in polycarbonate.

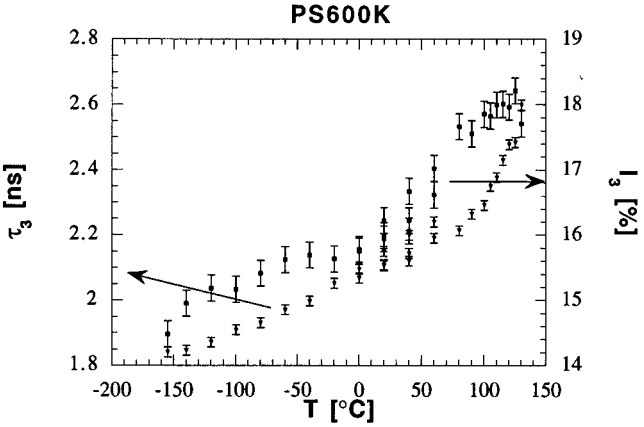

Figure 12. Temperature changes of the o-Ps lifetime and intensity in polystyrene.

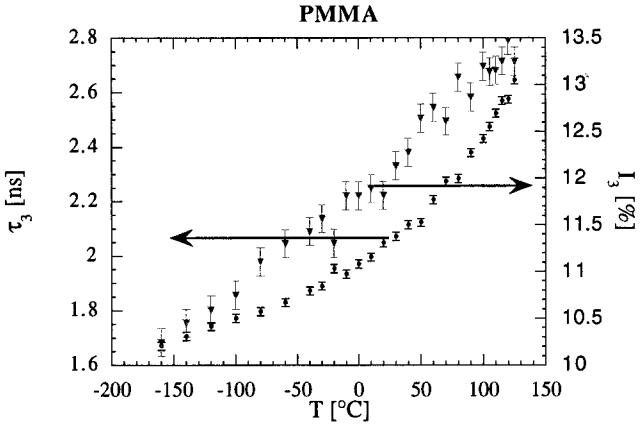

Figure 13. Temperature changes of the o-Ps lifetime and intensity in PMMA.

polymers. The overall changes of τ_3 are in the limits ~1.7−2.7 ns, which according to eq 1 corresponds to radius changes in the range ~2.6−3.4 Å. The volume of the "average" hole nearly doubles when the temperature is increased from −160 to +180 °C (~80−160 Å^3).

References and Notes

(1) Kaush, H.-H. *Polymer Fracture*; Springer-Verlag: Berlin, 1978.
(2) Schultz, J. M. *Solid State Behavior of Linear Polyesters and Polyamides*; Schultz, J. M., Fakirov, S., Eds.; Prentice Hall: Englewood Cliffs, NJ, 1990; Chapter 2.
(3) Struik, L. C. E. *Physical Aging in Amorphous Polymers and Other Materials*; Elsevier: Amsterdam, 1978.
(4) Yeh, G. S.; Geil, P. H. *J. Macromol. Sci., Phys.* **1967**, *B1*, 235; 251.
(5) Klement, J. J.; Geil, P. H. *J. Macromol. Sci., Phys.* **1971**, *B1*, 505; 535.
(6) Petrie, S. E. B. *J. Polym. Sci.* **1972**, *10*, 1255.
(7) Ali, M. S.; Sheldon, R. *J. Polym. Sci.* **1972**, *C38*, 97.
(8) Reninger, A. L.; Wicks, G. G.; Uhlmann, D. R. *J. Polym. Sci. Polym. Phys.* **1975**, *13*, 1247.
(9) McAlea, K. P.; Shultz, J. M.; Gardner, K. H.; Wignall, G. D. *Macromolecules* **1985**, *18*, 447.
(10) Laskowski, B. C.; Yoon, D. Y.; McLean, D.; Jaffe, R. L. *Macromolecules* **1988**, *21*, 1629.
(11) Cervinka, L.; Fisher, E. W.; Dettenmaier, M. *Polymer* **1991**, *32*, 12.
(12) Wang, S. J.; Jean, Y. C. In *Positron and Positronium Chemistry*; Shrader, D. M.; Jean, Y. C., Eds.; Elsevier: Amsterdam, 1988.
(13) Stevens, J. R. Probe and Label Techniques. In *Methods of Experimental Physics*; Fava, R. A. Ed. (Marton, L., Marton, C., Eds. in Chief); Academic: New York, 1980; p 371.
(14) Kluin, J. E.; Yu, Z.; Vleeshouwers, S.; McGervey, J. D.; Jamieson, A. M.; Simha, R.; Sommer, K. *Macromolecules* **1993**, *26*, 1853−1861.
(15) Tao, S. J. *J. Chem. Phys.* **1972**, *56*, 5499.
(16) Eldrup, M.; Lightbody, D.; Sherwood, J. N. *Chem. Phys.* **1981**, *63*, 51.
(17) Nakanishi, H.; Ujihira, Y. *J. Phys. Chem.*, **1982**, *86*, 4446.
(18) Nakanishi, H.; Wang, Y. Y.; Jean, Y. C.; Sandreczki, T. C.; Ames, D. P. In *Positron Annihilation in Fluids*; Sharma, S. C. Ed.; World Scientific: River Edge, NJ, 1988; p 78.
(19) Yu, Z.; Yahsi, U.; McGervey, J. D.; Jamieson, A. M.; Simha, R. *J. Polym. Sci. Polym. Phys.* **1994**, *32*, 2637.
(20) Serna, J.; Abbe, J. Ch.; Duplatre, G. *Phys. Stat. Sol.* (*A*) **1990**, *115*, 389.
(21) Doolittle, A. K. *J. Appl. Phys.* **1951**, *22*, 1471; **1952**, *23*, 236.
(22) Cohen, M. H.; Turnbull, D. *J. Chem. Phys.* **1959**, *31*, 1164.
(23) Turnbull, D.; Cohen, M. H.; *J. Chem. Phys.* **1961**, *34*, 120.
(24) McCrum, N. G.; Read, B. E.; Williams, G. *Anelastic and Dielectric Effects in Polymeric Solids*; Dover: New York, 1991; p 244.
(25) Xie, L.; Gidley, D. W.; Hristov, H. A.; Yee, A. F. *J. Polym. Sci. Polym. Phys.* **1995**, *33*, 77.
(26) van Krevelen, D. W. *Properties of Polymers*; Elsevier: Amsterdam, 1976.
(27) *Polymer Handbook*; Brandrup, J., Immergut, E. H., Eds.; Wiley: New York, 1989.
(28) Zoller, P. *J. Polym. Sci. Polym. Phys.* **1982**, *20*, 1453.
(29) Puff, W. *Compt. Phys. Commun.* **1983**, *30*, 359.
(30) Nakanishi, H. *Positron Annihilation in Liquids*; Sharma, S. C., Ed.; World Scientific Publishing: Singapore 1989.
(31) Kluin, J. E.; Yu, Z.; Vleeshouwers, S.; McGervey, J. D.; Jamieson, A. M.; Simha, R. *Macromolecules* **1992**, *25*, 5089.
(32) Jean, Y. C.; Yuan, J.-P.; Liu, J.; Deng, Q.; Yang, H. *J. Polym. Sci. Polym. Phys.* **1995**, *33*, 2365.
(33) Kristiak, J.; Bartos, J.; Kristiakova, K.; Sausa, O.; Bandzuch, P. *Phys. Rev. B* **1994**, *49*, 6601.
(34) Liu, J.; Deng, Q.; Jean, Y. C. *Macromolecules* **1993**, *26*, 7149.
(35) Bonart, R. *Makromol. Chem.* **1966**, *92*, 149.
(36) Kramer, E. J. *Adv. Polym. Sci.* **1983**, *52/53*, 1.
(37) Callen, H. B. *Thermodynamics*; Wiley: New York, 1960.
(38) Wendorff, J. H.; Fischer, E. W. *Kolloid Z. Z. Polym.* **1973**, *251*, 876.
(39) Rathje, J.; Ruland, W. *Colloid. Polym. Sci.* **1976**, *254*, 358.
(40) Fischer, E. W.; Hellmann, G. P.; Spiess, H. W.; Horth, F. J.; Ecarius, U.; Wehrle, M. *Macromol. Chem. Suppl.* **1985**, *12*, 189.
(41) Roe, R.-J.; Curro, J. J. *Macromolecules*, **1983**, *16*, 428.
(42) Egami, T.; Srolovitz, D. *J. Phys.* **1981**, *F11*, 2209.
(43) Srolovitz, D.; Maeda, K.; Vitek, V.; Egami, T. *Phil. Mag.* **1981**, *44*, 847.
(44) Kittel, Ch. *Introduction to Solid State Physics*; Wiley: New York, 1986, pp 92.

MA960719K